Changes in stellar spin by the magnetic field structure inside the accretion disk

or

Missing component in the star-disk interaction torque

Miljenko Čemeljić

College of Astronomy and Natural Sciences, SGMK
Nicolaus Copernicus Superior School, Warsaw, Poland
&
Nicolaus Copernicus Astronomical Center, PAN
Warsaw, Poland (CAMK)
&
Institute of Physics, Silesian University in Opava, Czech Republic

With Włodek Kluźniak from CAMK

Outline

- Introduction, analytical solutions for thin accretion disk
- Numerical simulations of thin accretion disk in non-ideal MHD
- “Atlas” (2019) and “Trends” (2023) papers with solutions and analysis.
- Magnetic field inside the disk and missing component in computation of torque on the star.
- Summary

Introduction

•We still lack understanding of stellar slow-down during the star formation or for pulsars.

•First numerical solution of (HD) accretion disk was by Prendergast & Burbidge (1968), followed by most cited solution by Shakura & Sunyaev (1973), introducing a parameter alpha in which are hidden unknowns about turbulence.

•In David Kita's (1995, PhD Thesis) and Kluźniak & Kita (2000, KK00 hereafter) was given a solution of the thin HD polytropic disk in the full 3D. It was obtained by the method of asymptotic approximation with the disk thickness as a small parameter for axisymmetric case.

•In 2009, numerical simulations of star-disk magnetospheric interaction were performed in

2D-axisymmetric simulations, by Romanova et al. (2009, 2013, with a non-public code) and in Zanni & Ferreira (2009, 2013), with the publicly available PLUTO code.

•In Čemeljić, 2019, **"Atlas"** paper, I repeated the Zanni et al. (2009) 2D axisymmetric viscous & resistive MHD simulations with PLUTO (ver. 4.1). I went on to perform a parameter study, to investigate dependence of solution on different parameters (Čemeljić & Brun, 2023, **"Trends"** paper).

•We compared numerical solutions with analytical results in Čemeljić, Kluźniak & Parthasarathy, 2023.

•With the same setup, in our group in Warsaw we also investigated simulations with meridional backflow (Mishra, Čemeljić & Kluźniak, 2023), axial outflows (Kotek et al, 2020) and non-dipolar stellar magnetic field (Cieciuch & Čemeljić, 2022, for quadrupole, octupole and mixed field).

Numerical setup

•To compute torques on the star, we need simulations with star-disk magnetospheric interaction. I perform simulations with a thin Kluźniak-Kita accretion disk, which reach a quasi-stationary state.

•Ohmic and viscous heating in the energy equation are extracted, assuming that all the heat is radiated away.

•Viscosity and resistivity are still included, in the equation of motion and in the induction equation.

$$\frac{\partial \rho}{\partial t} + \nabla \cdot (\rho \boldsymbol{u}) = 0$$

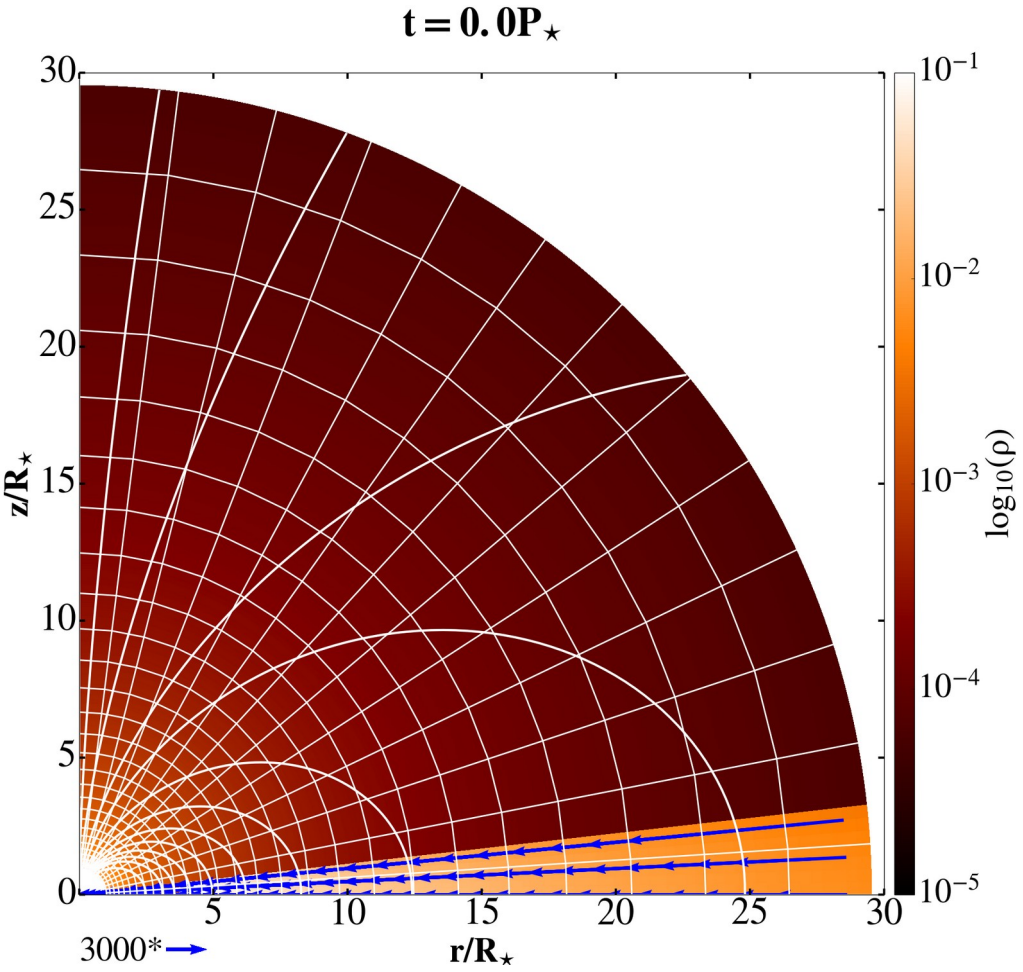
$$\frac{\partial \rho \boldsymbol{u}}{\partial t} + \nabla \cdot \left[\rho \boldsymbol{u}\boldsymbol{u} + \left(P + \frac{\boldsymbol{B} \cdot \boldsymbol{B}}{8\pi} \right) \boldsymbol{I} - \frac{\boldsymbol{B}\boldsymbol{B}}{4\pi} - \boldsymbol{\tau} \right] = \rho \boldsymbol{g}$$

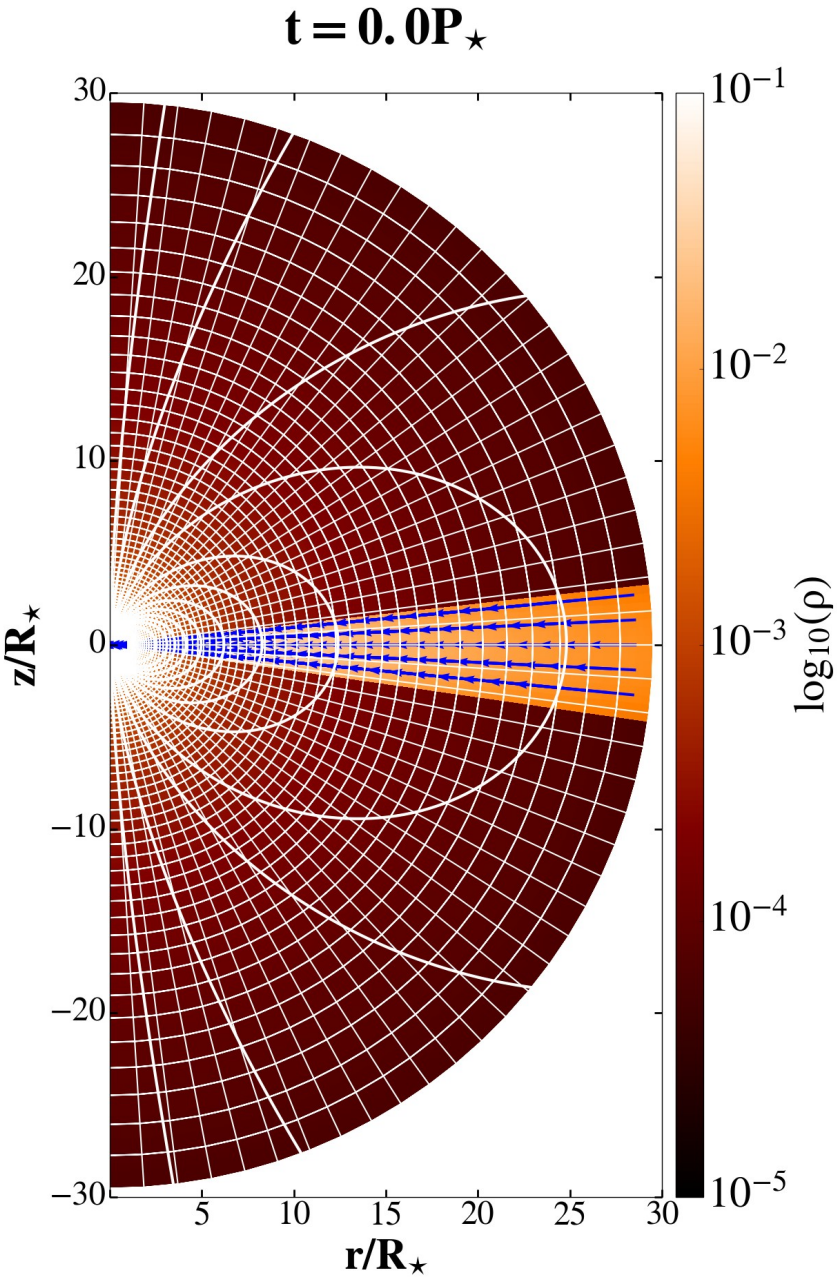
$$\frac{\partial E}{\partial t} + \nabla \cdot \left[\left(E + P + \frac{\boldsymbol{B} \cdot \boldsymbol{B}}{8\pi} \right) \boldsymbol{u} - \frac{(\boldsymbol{u} \cdot \boldsymbol{B})\, \boldsymbol{B}}{4\pi} \right]$$
$$+ \nabla \cdot [\eta_{\mathrm{m}} \boldsymbol{J} \times \boldsymbol{B}/4\pi - \boldsymbol{u} \cdot \boldsymbol{\tau}] = \rho \boldsymbol{g} \cdot \boldsymbol{u} - \Lambda_{\mathrm{cool}}$$

$$\frac{\partial \boldsymbol{B}}{\partial t} + \nabla \times (\boldsymbol{B} \times \boldsymbol{u} + \eta_{\mathrm{m}} \boldsymbol{J}) = 0.$$

• Code was PLUTO (v.4.1) by Mignone et al. (2007). In 2025, with PhD student Sukalpa Kundu in Warsaw, we transferred the setup and performed the same simulations in the latest version of PLUTO (v. 4.4. patch 4). A non-trivial task, as the code changed much, but it also improved.

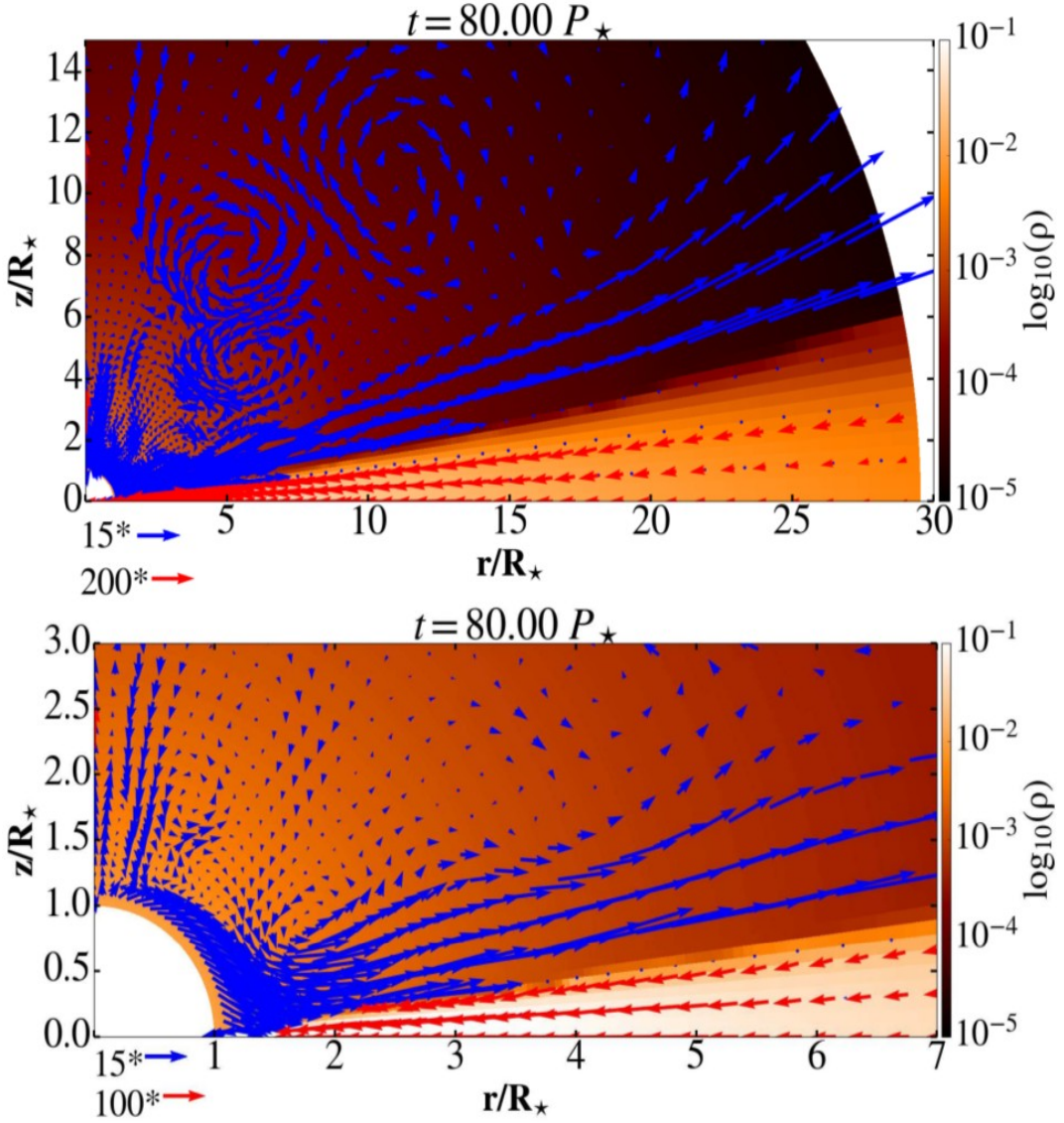
Star-disk simulations with magnetic field



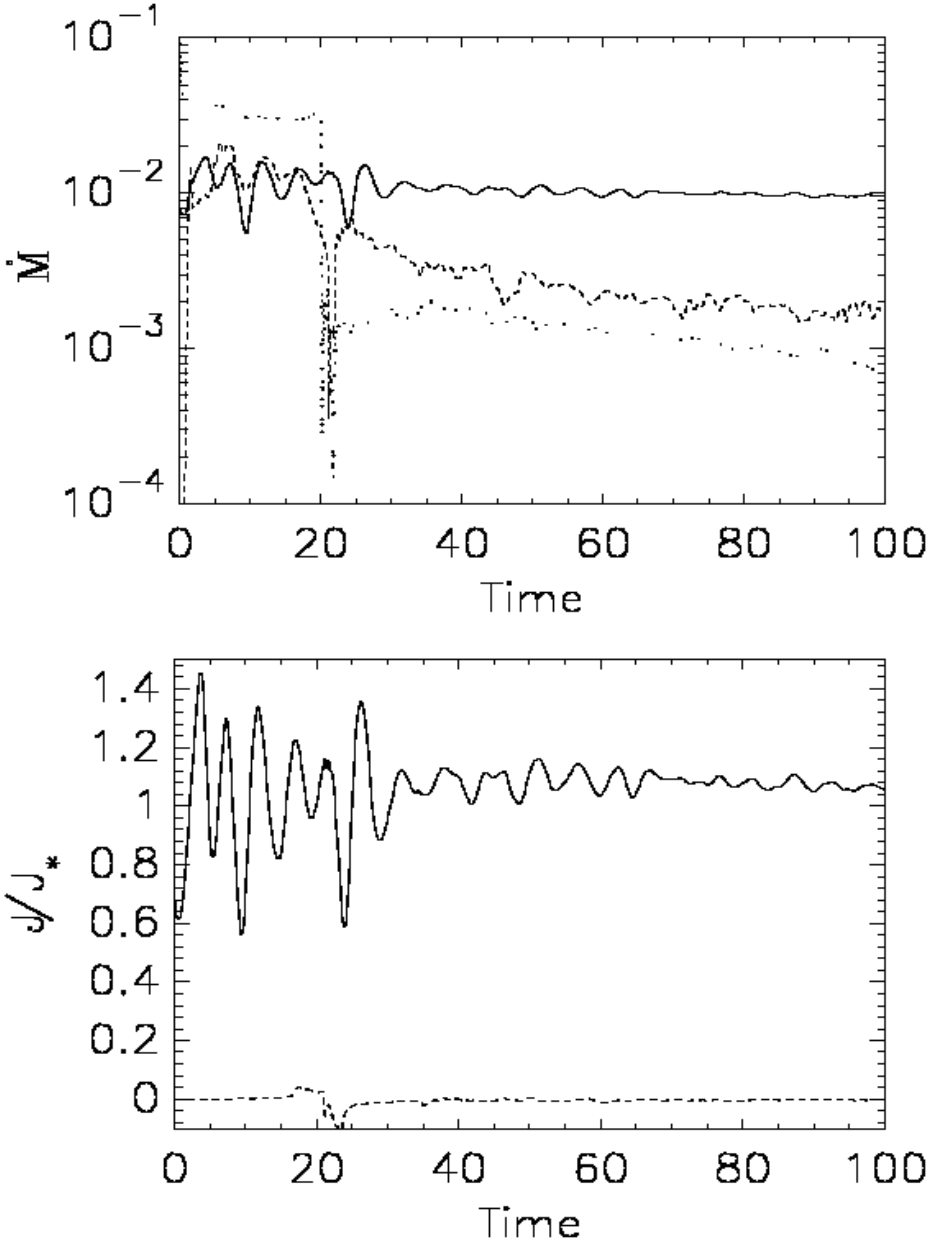


- First we perform purely HD simulations and then we add the magnetic field to the HD solution.
- We assume the star to be a magnetized rotator. Stellar surface is a rotating boundary condition at the origin of the spherical computational domain. The initially non-rotating corona is in a hydrostatic balance. After a few stellar rotations it corotates with the disk.

Hydro-dynamic SDI simulations



Computational box and a zoom closer to the star after 80 stellar rotations. In color is shown the density, and vectors show velocity, with the different normalization in the disk and stellar wind.



Time dependence of the mass and angular momentum fluxes in the various components in our simulations.

Star-disk magnetospheric interaction simulations with α_v=1.

Table 1. The parameters in our study presented in the "Atlas": the stellar angular velocity $\Omega_\star$, stellar dipole magnetic field strength $B_\star$, and the magnetic Prandtl number P_m-for which we also table the values of corresponding resistivity coefficient α_m. We show also the stellar rotation period, and corotation radius in young stellar object (YSO) cases.

$\Omega_\star/\Omega_\mathrm{br}$	$B_\star$(G)	P_m	α_m	$P_\star$(days)	$R_\mathrm{cor}(R_\star)$
0.05	250	6.7	0.1	9.2	7.37
0.1	500	1.67	0.4	4.6	4.64
0.15	750	0.95	0.7	3.1	3.54
0.2	1000	0.67	1.0	2.3	2.92

- Prandtl magnetic number: $P_\mathrm{m} = \frac{2}{3}\frac{\alpha_\mathrm{v}}{\alpha_\mathrm{m}}$

- With PhD students and with summer students, we continued work, to go to the other parts of the parameter space and other geometries of magnetic field. Such 2D axisymmetric results are needed, for a comparison with theoretical predictions.
- The work in full 3D is under way, I showed it in the last RAGTIME.

Analysis of "Atlas" solutions

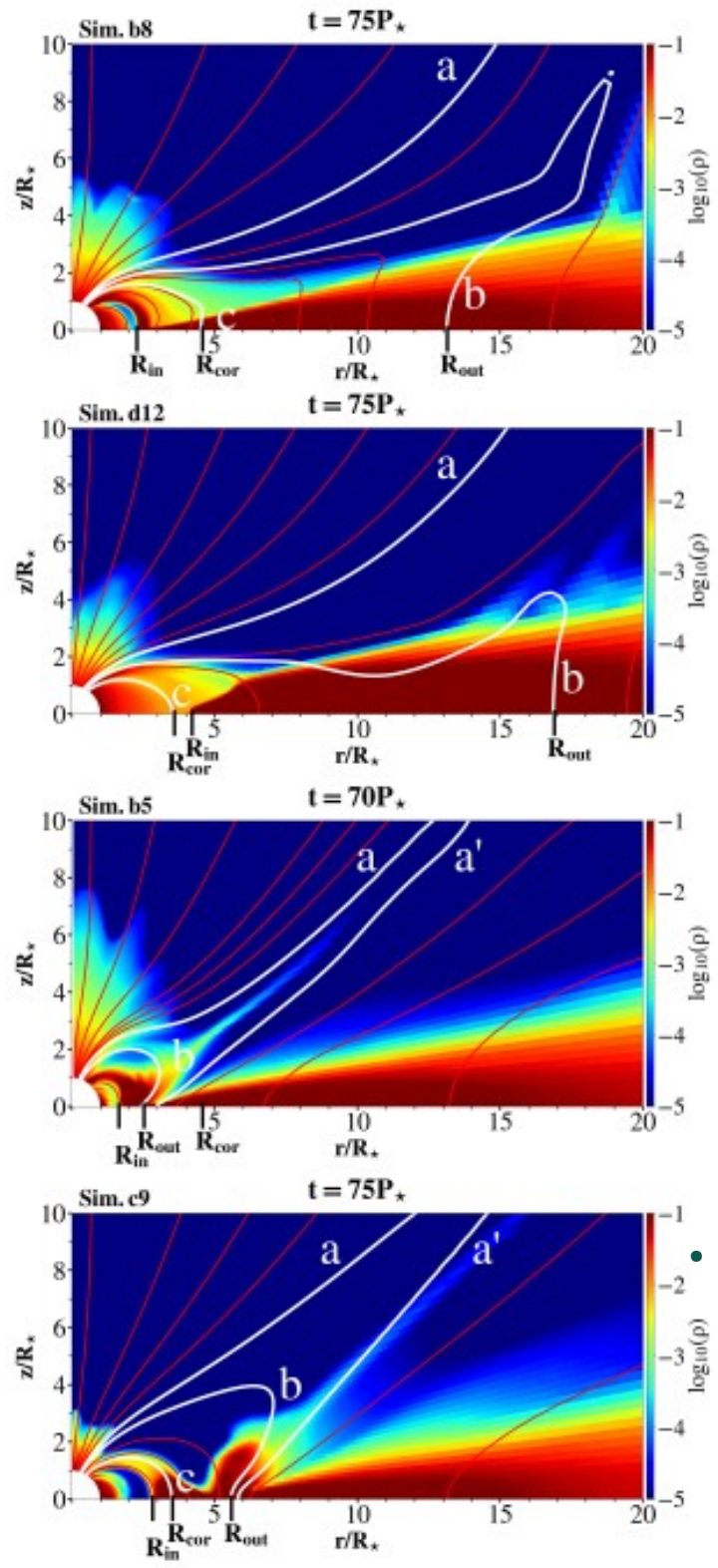
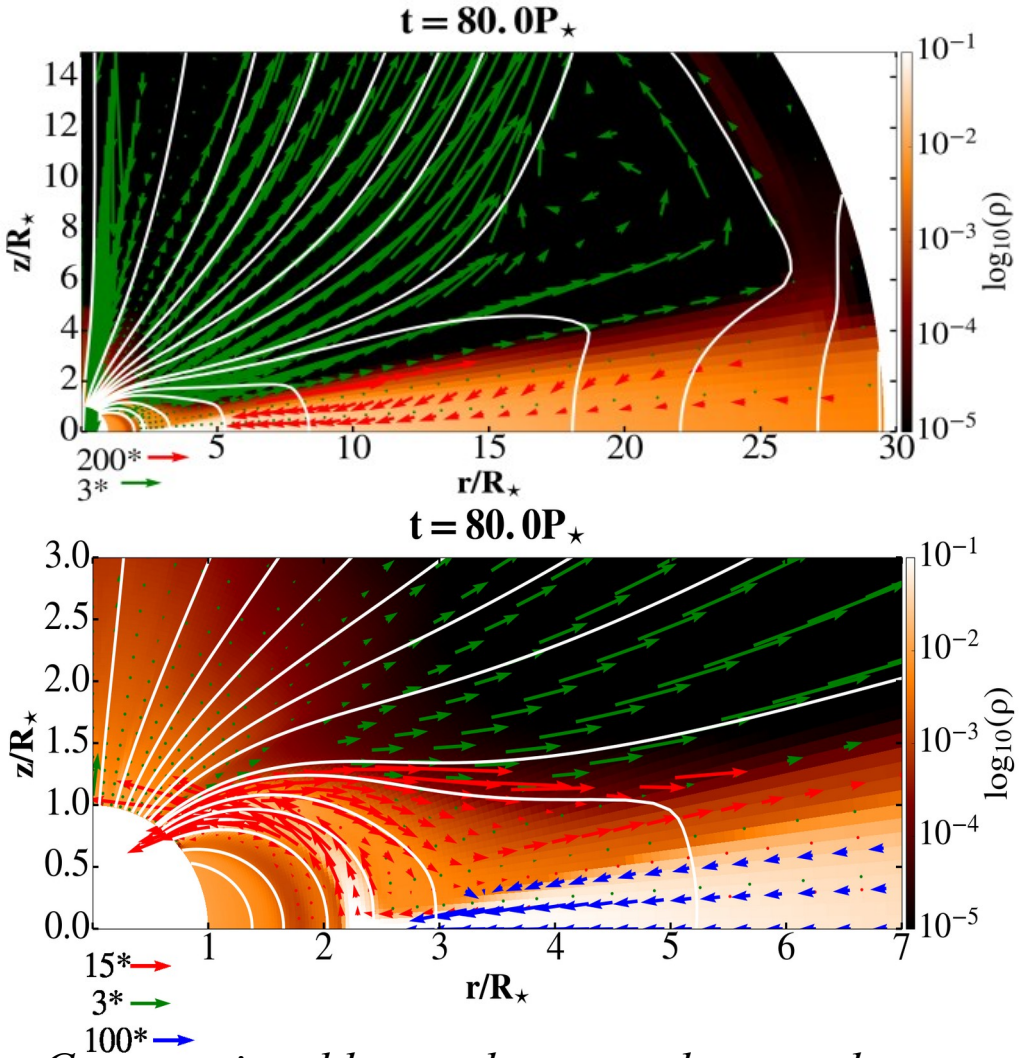


Table 1. 64 star-disk magnetospheric interaction simulations in a setup detailed in Čemeljić (2019).

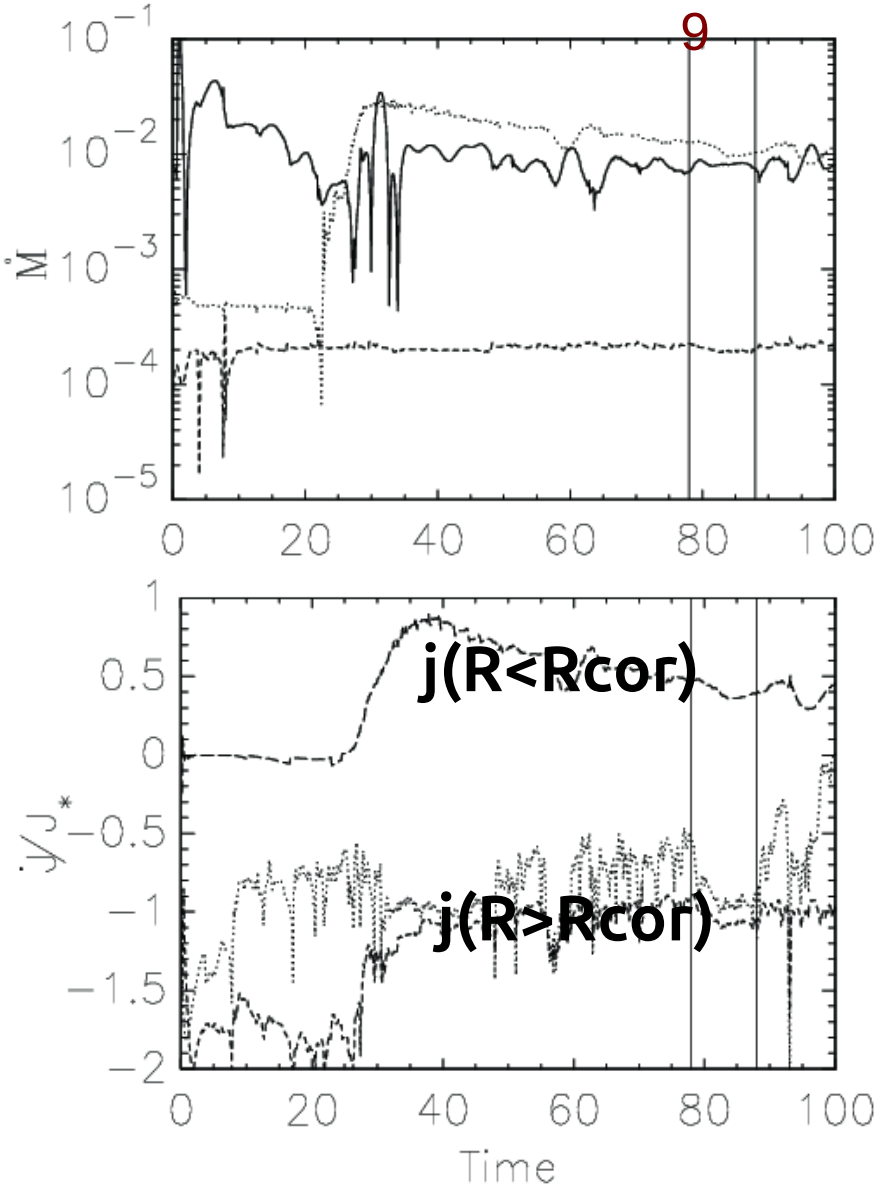
α_m =	0.1	0.4	0.7	1
P_m =	6.7	1.67	0.95	0.67
$\Omega_\star/\Omega_{br}$				
		$B_\star$ = 250 G		
0.05	**a1**(DCE1)	**a2**(DC)	**a3**(DC)	**a4**(DC)
0.1	**a5**(DCE1)	**a6**(DC)	a7(DC)	**a8**(DC)
0.15	**a9**(DCE1)	**a10**(DC)	a11(DC)	**a12**(DC)
0.2	a13(DCE1)	a14(DC)	a15(DC)	a16(DC)
		$B_\star$ = 500 G		
0.05	**b1**(DCE1)	**b2**(DC)	**b3**(DC)	**b4**(DC)
0.1	**b5**(DCE1)	b6(DC)	b7(DC)	b8(DC)
0.15	**b9**(DCE1)	b10(DC)	b11(DC)	b12(DC)
0.2	b13(DCE1)	b14(DC)	b15(DC)	b16(DC)
		$B_\star$ = 750 G		
0.05	**c1**(DCE1)	c2(DC)	**c3**(DC)	c4(DC)
0.1	**c5**(DCE1)	c6(DC)	c7(DC)	c8(DC)
0.15	c9(DCE2)	c10(DC)	c11(DC)	c12(DC)
0.2	c13(DCE2)	c14(DC)	c15(DC)	c16(DC)
		$B_\star$ = 1000 G		
0.05	**d1**(DCE1)	d2(DC)	**d3**(DC)	d4(DC)
0.1	**d5**(DCE1)	d6(DC)	d7(DC)	d8(DC)
0.15	d9(DCE2)	d10(D)	d11(D)	d12(D)
0.2	d13(DCE2)	d14(D)	d15(D)	d16(D)

- I did a systematic study with magnetic star-disk numerical simulations in 64 points in parameter space, for a slowly rotating star. With respect to the position of Rcor (in the case with conical outflow), I found 4 different cases of solutions. In general, faster stellar rotation prevents fotmation of the accretion column. In the two bottom panels resistivity αm=0.1, always resulting in magnetospheric ejection (conical outflow).

Mass and angular momentum fluxes in simulations of magnetospheric interactio



Computational box and a zoom closer to the star after 80 stellar rotations, to visualize the accretion column and the magnetic field lines (white solid lines), connected to the disk beyond the corotation radius Rcor=2.92 Rs. In color is shown the density, and vectors show velocity, with the different normalization in the disk, column and stellar wind.



Time dependence of the mass and angular momentum fluxes in the various components in our simulations with marked the time interval in which the average for the quasi-stationarity is computed.

Comparison of SDMI simulations with increasing mag. field

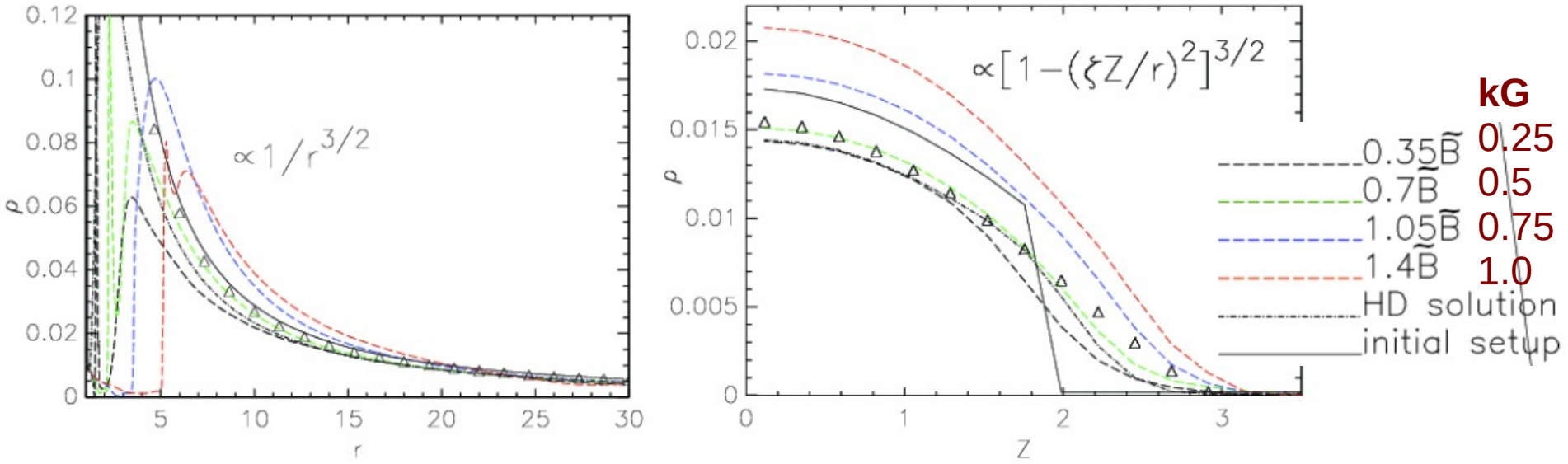


Fig. 3. Comparison of the matter density *Left panel:* radial dependence along the midplane, just above θ=90°. *Right panel:* the profiles along the vertical line at r=15$R_\star$. The legend is the same as in Fig. 2.

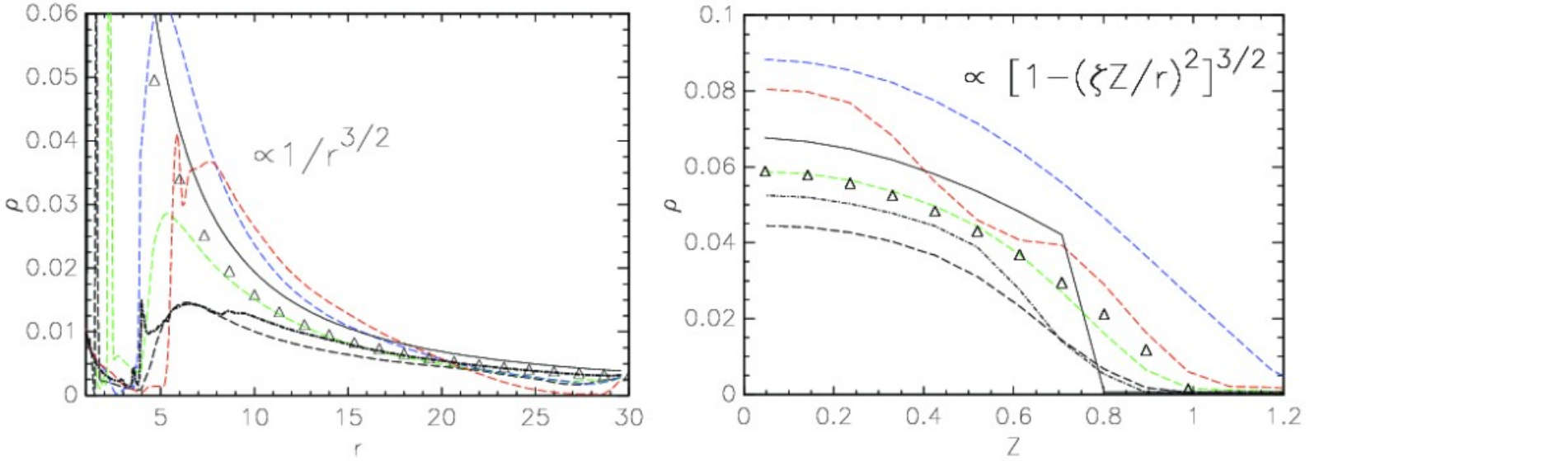
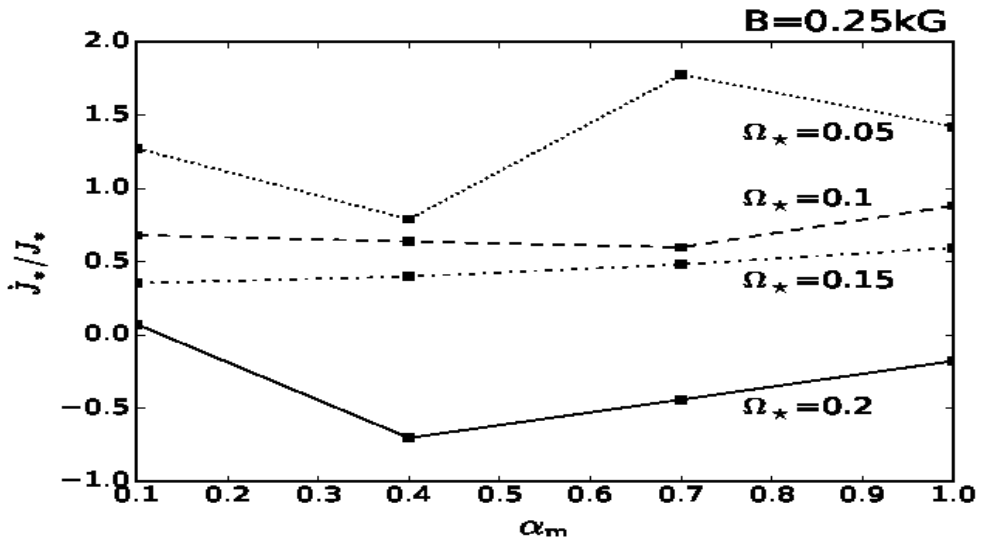
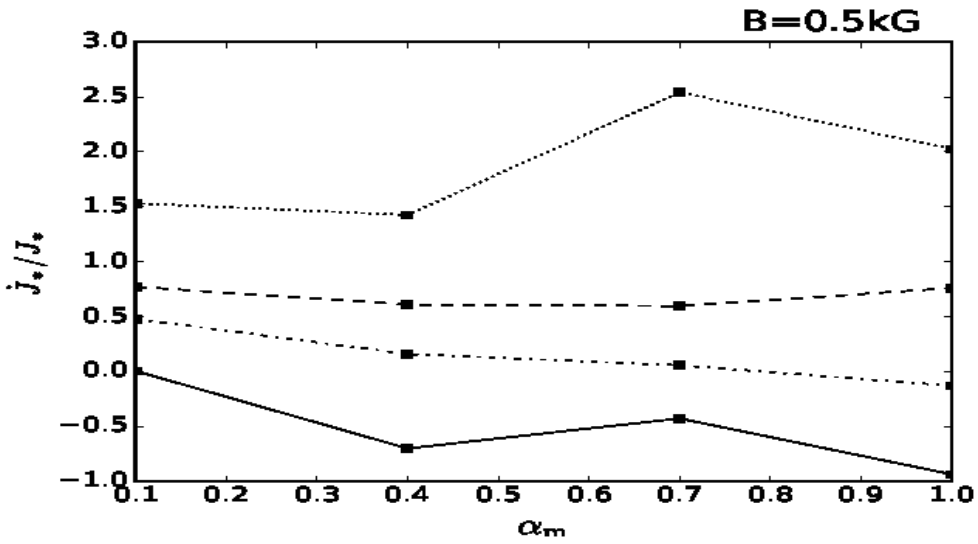
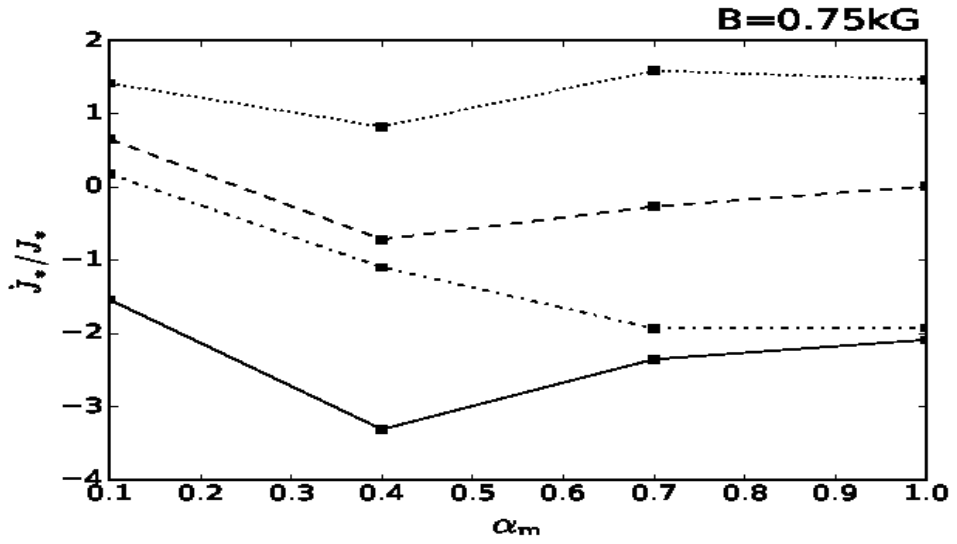


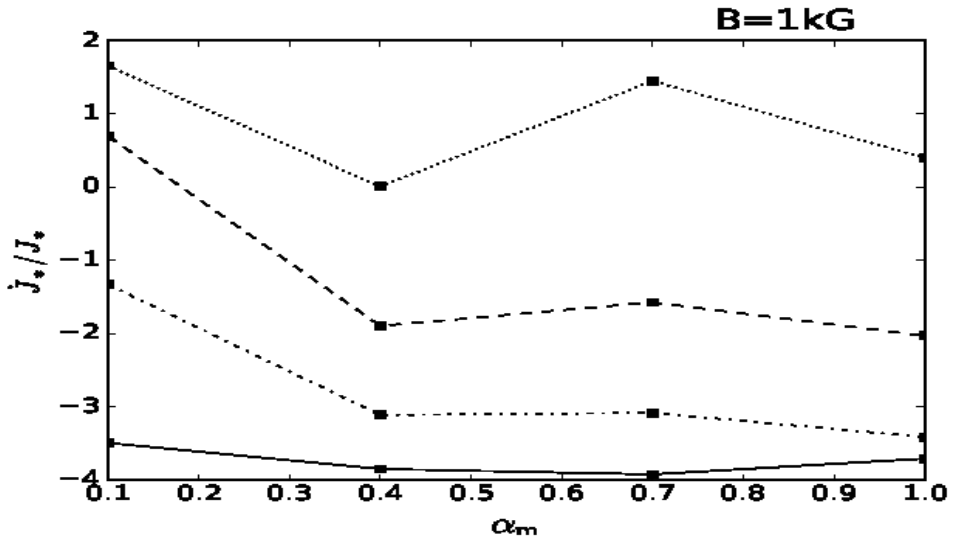
Fig. 4. Comparison of the matter density in the initial set-up (solid line) with the quasi-stationary solutions in numerical simulations in the HD (dot-dashed line) and the MHD cases. *Left panel:* along the disc surface at θ=83°. *Right panel:* along a vertical line at r=6$R_\star$. The meaning of the lines is the same as in Fig. 3.

Trends in angular momentum with increasing stellar magnetic field









Average angular momentum flux transported onto the stellar surface by the matter in-falling from the disk onto the star through the accretion column. In each panel is shown a set of solutions with one stellar magnetic field strength, varying the stellar rotation rate and resistivity. Positive flux spins-up the star, negative slows it down. With the increase in stellar rotation rate, spin-up of the star by the infalling matter decreases, eventually switching to the spin-down.c

Torques with the disk field included in the computation

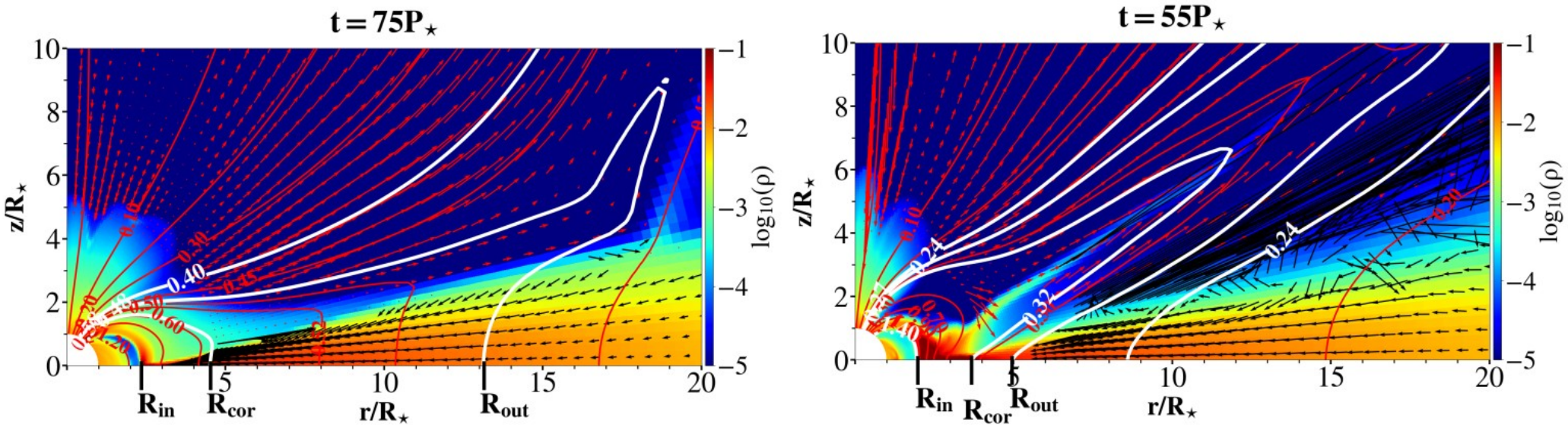


Fig. 1. Density in a logarithmic color grading in snapshots from quasi-stationary solutions in two cases in our numerical simulations with anomalous viscosity parameter $\alpha_v = 1.0$. In the left panel is shown solution with anomalous resistivity $\alpha_m = 1.0$ and stellar magnetic field and rotation rate $B_\star = 0.5$ kG, and $\Omega_\star$=0.1 Ω_{br}, respectively. In the right panel is shown the solution with $\alpha_m = 0.1$, $B_\star = 0.75$ kG and $\Omega_\star$=0.15 Ω_{br}. A sample of magnetic field lines is shown with red solid lines. White solid lines are delimiting the components of the flow between which we integrate the fluxes. Vectors representing the poloidal velocity are normalized to Keplerian velocity on the stellar equator and the velocities in the disk multiplied with constant factors of the order of 100 to be visible in the plot.

Torque on the star is usually computed from the matter infalling on the star plus viscous and magnetic components, with integrals taken between the thick white lines:

$$\boldsymbol{F}_{\rm Lm} = r\sin\theta\rho v_\phi \boldsymbol{v}_{\rm p}, \qquad \boldsymbol{F}_{\rm Lf} = -r\sin\theta\frac{B_\phi \boldsymbol{B}_{\rm p}}{4\pi},$$

$$\boldsymbol{F}_{\rm Lv} = -\nu_{\rm t}\rho(r\sin\theta)^2\nabla\Omega. \qquad \dot{J}_\star = \int_{\rm S}\left[R\rho v_\varphi \boldsymbol{v}_{\rm p} - \nu\rho(R\sin\theta)^2\nabla\Omega - \frac{RB_\varphi \boldsymbol{B}_{\rm p}}{4\pi}\right]d\boldsymbol{S},$$

Torques with the magnetic field inside the disk

In Naso & Miller (2010, 2011) and Naso et al. (2013) the torques were for the first time computed with the magnetic field inside the disk taken into account. They did not have the disk solutions, so they had to assume some profiles. With our solutions, we can check their results.

Their conclusion was that different vertical zones inside the disk may spin-up or spin-down the central star, regardless of the position of the corotation radius, at which the material in the disk corotates with the stellar surface.

The expression for magnetic torque is:

$$\boldsymbol{T}_{B-disk} = \int_V \boldsymbol{R} \times \boldsymbol{F}_L dV.$$

$$\boldsymbol{F}_{\mathrm{L}} = \frac{1}{c}\boldsymbol{J} \times \boldsymbol{B} = \frac{\nabla \times \boldsymbol{B}}{4\pi} \times \boldsymbol{B}.$$

The azimuthal component:

$$F_\varphi = \frac{1}{4\pi}\frac{B_\theta}{R\sin\theta}\frac{\partial}{\partial\theta}(B_\varphi \sin\theta) + \frac{1}{4\pi}\frac{B_R}{R}\frac{\partial}{\partial R}(RB_\varphi) - \frac{1}{4\pi}\frac{1}{R\sin\theta}\left(B_\theta\frac{\partial B_\theta}{\partial\varphi} + B_R\frac{\partial B_R}{\partial\varphi}\right).$$

In the axisymmetric case the last two terms are zero, so we have:

$$\boldsymbol{T}_{B-disk} = \int_V RF_\varphi\hat{\theta}dV = -2\pi\int_R\int_\theta RF_\varphi R^2\sin\theta dRd\theta\hat{\boldsymbol{z}}.$$

$$\boldsymbol{T}_{B-disk} = \int_R\int_\theta -\frac{R^2}{2}\left[B_\theta\frac{\partial}{\partial\theta}(B_\varphi\sin\theta) + B_R\frac{\partial}{\partial R}(RB_\varphi)\sin\theta\right]dRd\theta\hat{\boldsymbol{z}}.$$

Components of the magnetic field

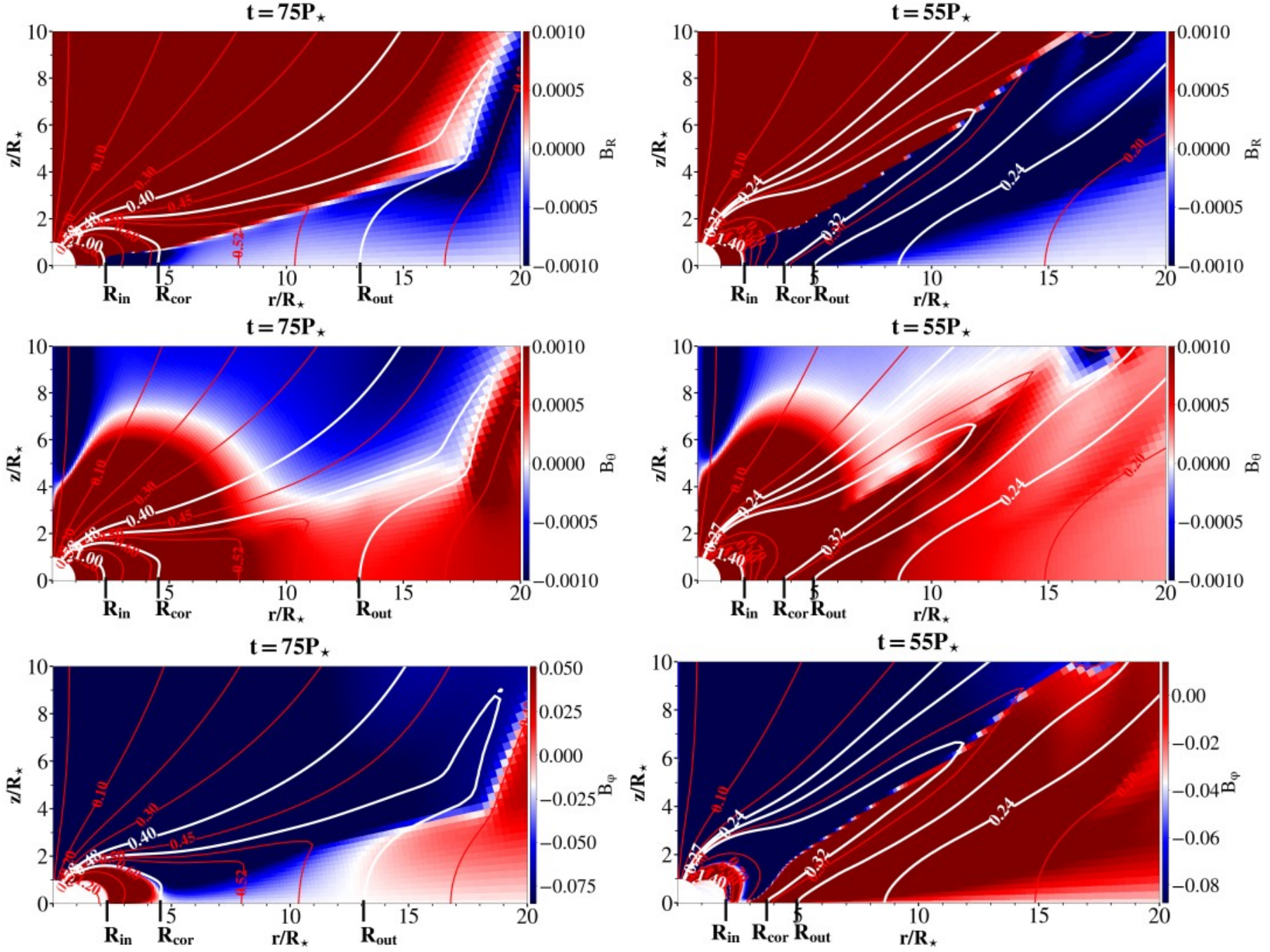
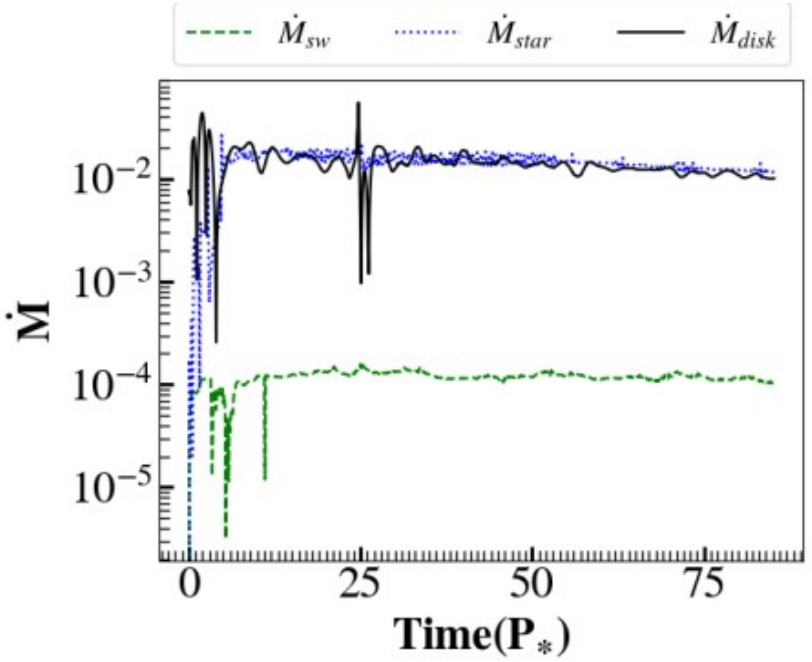
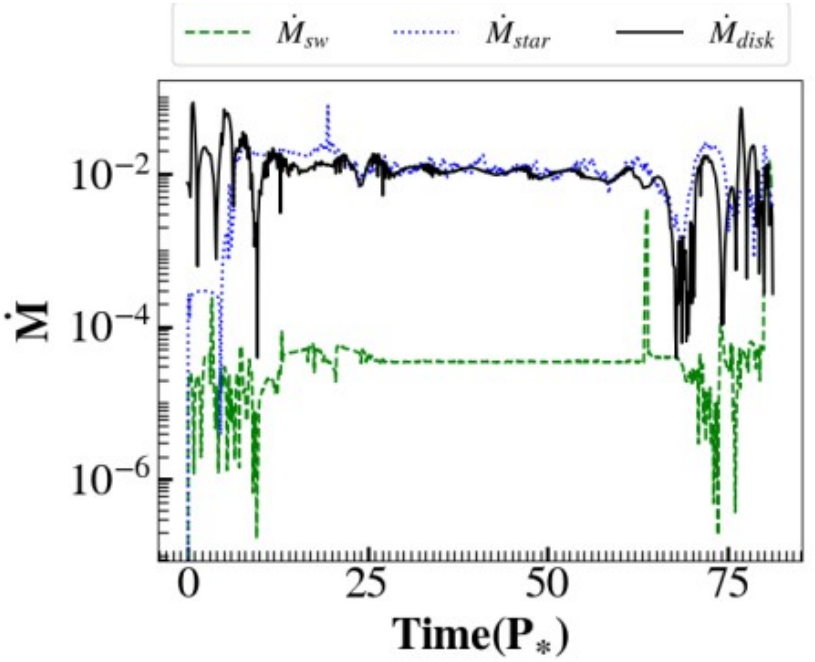
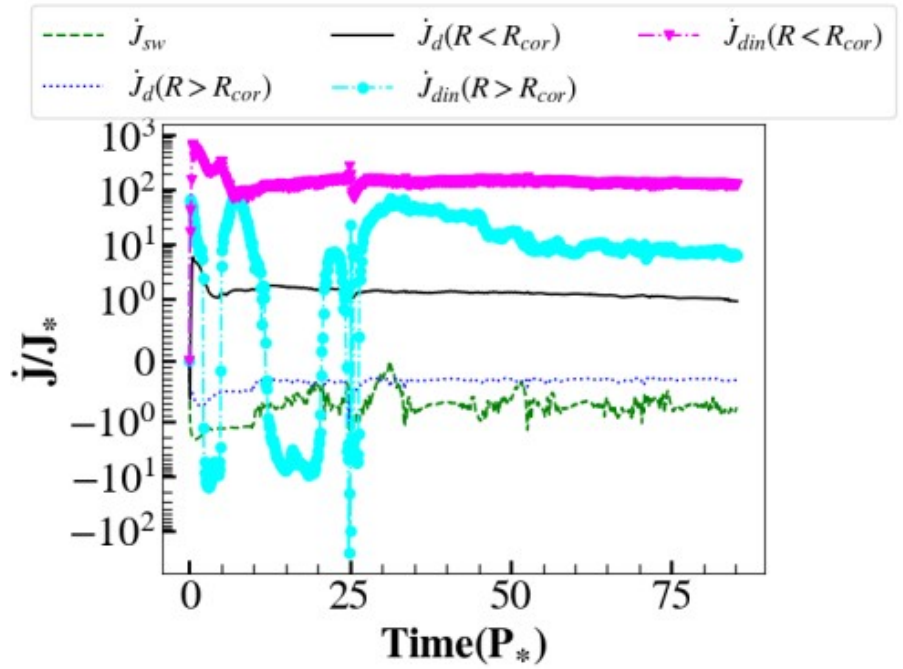


Fig. 2. Components of the magnetic field in the two cases from Figure 1.







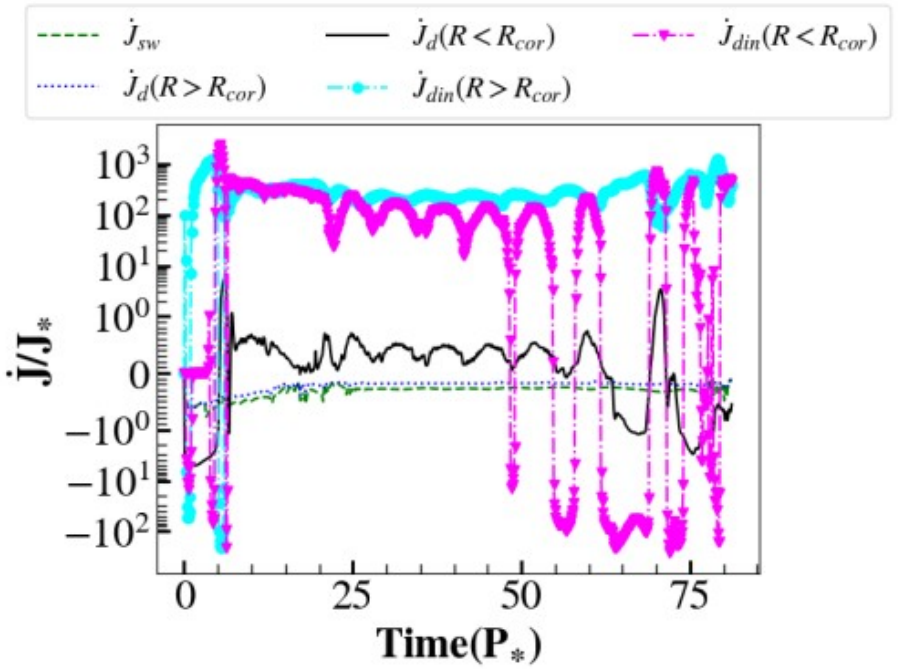


Fig. 5. Mass fluxes and torques on the star in the solution without magnetospheric ejection.

Fig. 6. Mass fluxes and torques on the star in the solution with magnetospheric ejection.

Mass fluxes and torques

In the quasi-stationary interval torque can be not so stationary in some cases:

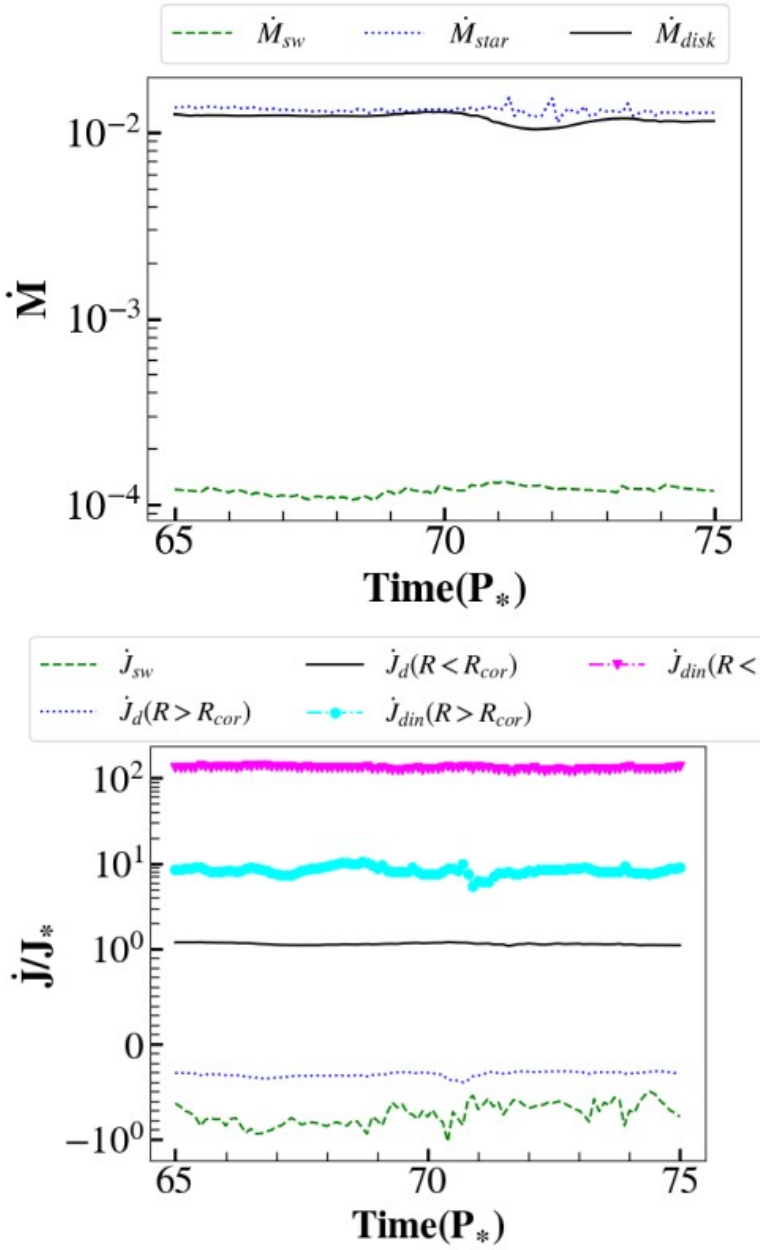


Fig. 3. Mass fluxes and torques on the star in the solution without magnetospheric ejection.

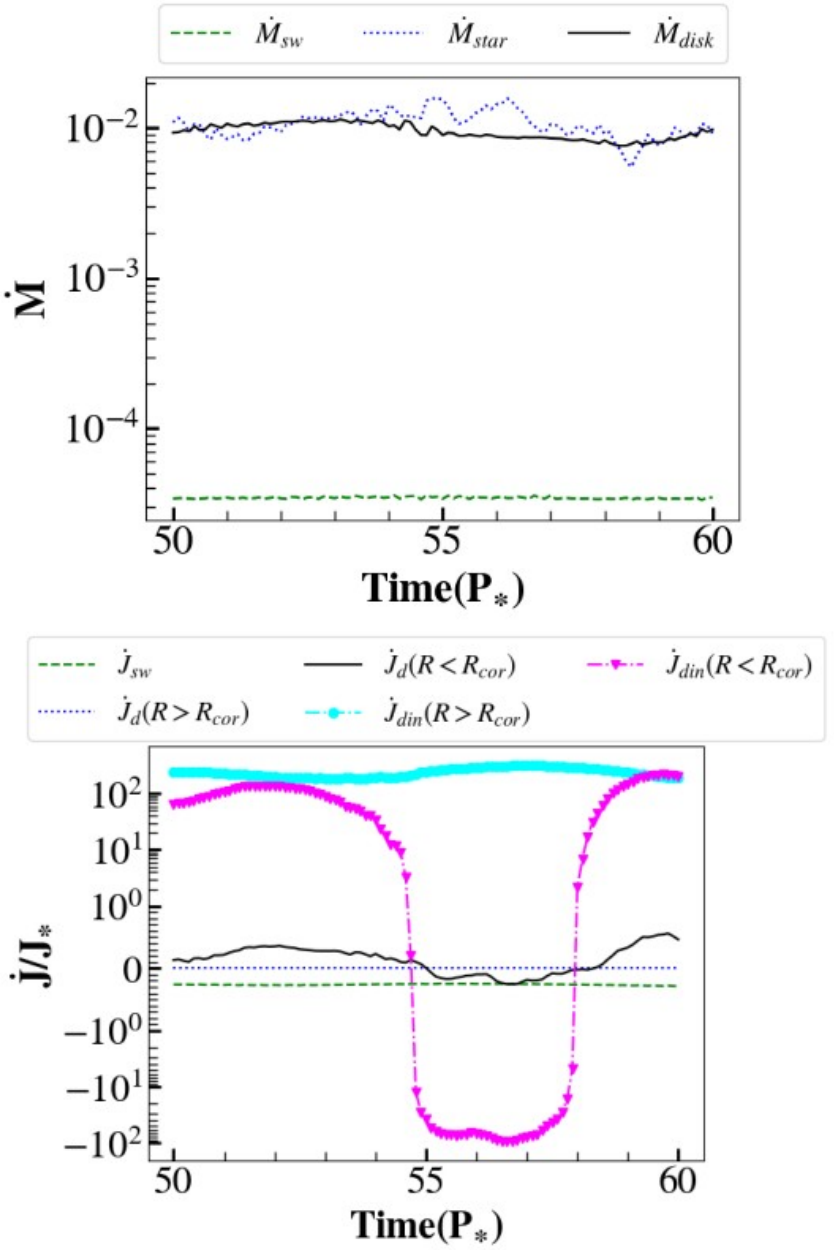


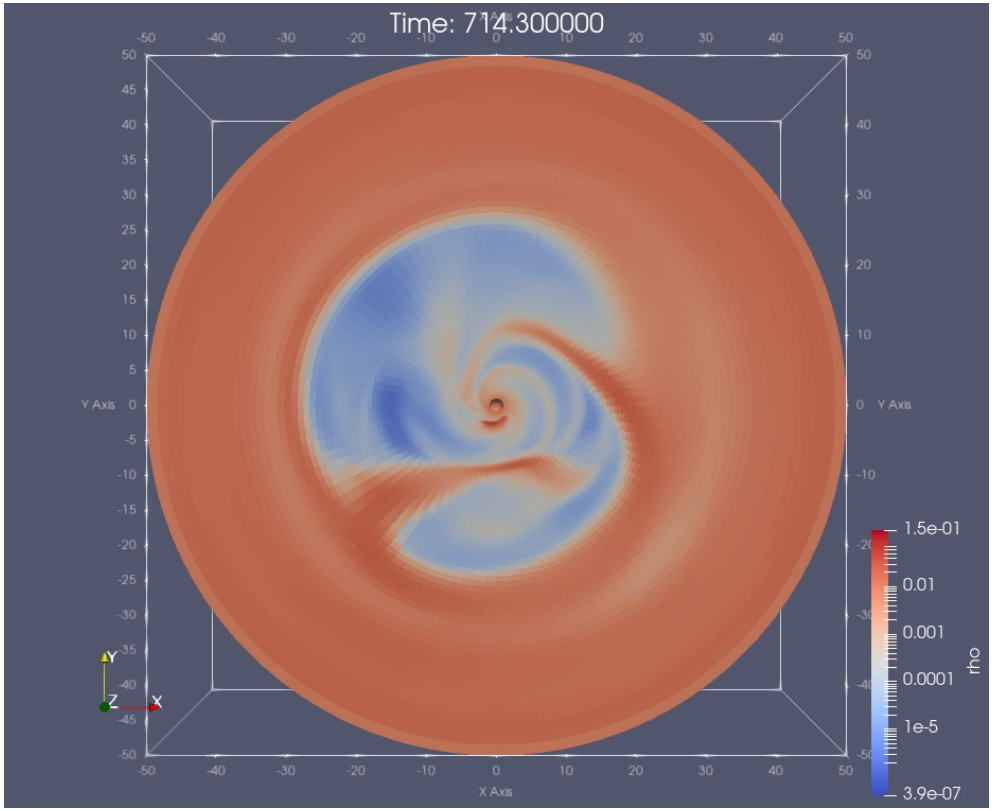
Fig. 4. Mass fluxes and torques on the star in the solution with magnetospheric ejection.

Summary

-The purely hydro-dynamic analytical solutions for a thin disk are available in Kluźniak & Kita 2000. We use them as the initial state for magnetic simulations.

-We obtained a quasi-stationary state in a parameter study with 64 viscous and resistive MHD simulations with slowly rotating stars (up to 0.2 of the breakup stellar rotation rate). They are re-scalable to YSOs, WDs and NSs. Results can be compared to find trends for angular momentum in the solutions.

-We also computed the torques with the magnetic field inside the disk taken into account. There are huge differences, and in some cases, this changes the qualitative picture.



In full 3D, with spirals in the magnetized disk, it becomes even more interesting!

Work is in progress!